Croatian Society for Materials Protection

Metalurgija/Metallurgy

Vol. 65 No. 3 / 2026

Microstructural and Mechanical Modification of Ductile Iron by Niobium Addition

César Becerra [1*], Felipe Hernández [2], Jesús García [1], Zianya Gómez [1] and Marissa Vargas [1*]

https://doi.org/10.64486/m.65.3.1

[1] Área Académica de Ciencias de la Tierra y Materiales, Universidad Autónoma del Estado de Hidalgo, Hidalgo, México; be260308@uaeh.edu.mx; jserrano@uaeh.edu.mx; go242872@uaeh.edu.mx; marissav@uaeh.edu.mx

[2] Escuela Superior de Ingeniería Mecánica y Eléctrica, Instituto Politécnico Nacional, Ciudad de México, México; fhernandezs@ipn.mx

* Correspondence: CB be260308@uaeh.edu.mx; MV marissav@uaeh.edu.mx.

Type of the Paper: Article

Received: July 25, 2025

Accepted: December 15, 2025

Abstract: This study investigated the influence of niobium additions on ductile iron through the production of four alloys containing 0 wt.%, 0.11 wt.%, 0.23 wt.% and 0.32 wt.% Nb. Microstructural phases were characterized, and mechanical properties were evaluated through hardness, impact toughness, tensile and wear tests. Niobium promoted carbide formation, which increased from 0.53 % to 2.48 %, and reduced graphite nodularity from 256.1 nod/mm² to 156.4 nod/mm². Hardness increased from 13.72 HRC to 26.6 HRC, while the ultimate tensile strength and yield strength reached 746 MPa and 449 MPa, respectively, in Alloy 4. In contrast, impact toughness decreased from 10.45 J to 5 J. Overall, niobium improved wear resistance but reduced the toughness of the material.

Keywords: niobium; ductile iron; pearlite; cementite

1. Introduction

Ductile irons are cast irons in which graphite solidifies in a nodular morphology, providing enhanced strength compared to flake graphite irons [1]. They are extensively used in gears, crankshafts, shafts and rolling cylinders due to their balanced combination of hardness, strength, ductility and impact toughness [2–3]. Over the years, different grades of ductile irons have been developed to improve their mechanical properties, making them competitive with steels [4].

Niobium additions induce changes in microstructure and, consequently, in mechanical performance. Previous studies have shown that additions above 2 wt.% Nb promote substantial improvements in mechanical properties [5]. It has been reported that niobium levels greater than 0.2 wt.% increase the pearlite fraction and refine its morphology by reducing the interlamellar spacing [6]. Additions of about 0.8 wt.% lead to the formation of polygonal NbC particles up to 8 μm in size [7], while Zhou et al. [8] observed that 1.48 wt.% Nb enhances hardness and wear resistance through the formation of elongated NbC particles with dimensions of approximately 10 μm. Cantera et al. [9] found that a 0.2 wt.% addition slightly reduced graphite nodularity in hypoeutectic ductile iron, though within acceptable limits. Fras et al. [10] reported that small additions (>0.038 wt.%) decreased nodule count and nodule diameter, improving ultimate tensile strength (UTS) and yield strength (YS). Other studies indicated that 0.47 wt.% Nb increased yield strength by up to 20 %, with only minor improvements in toughness relative to niobium-free ductile irons [11]. Overall, niobium generally enhances

tensile strength but may reduce ductility [12]. For instance, Pimentel et al. [13] observed a decrease in elongation from 7.8 % to 2.2 % in alloys containing 0 wt.%, 1 wt.% and 1.8 wt.% Nb.

The aim of this study is to evaluate the effect of small niobium additions on the microstructure and graphite morphology of ductile irons and to assess their influence on hardness, toughness, wear resistance, tensile strength and elongation.

2. Materials and Methods

To produce the four ductile iron alloys, a 30 kg Faraday induction furnace was used to melt AISI 1018 steel, graphite, ferrosilicon and ferroniobium. Inoculation and nodularization were carried out in the pouring ladle using ferrosilicon magnesium and ferrosilicon to ensure graphite precipitation in nodular form. The molten metal was then poured into ingot molds with dimensions of 130 × 500 × 100 mm. The chemical compositions of the alloys are given in Table 1 and were determined using a Shimadzu Spark PDA-7000 spectrometer as the average of five measurements taken from different regions of each sample.

For metallographic analysis, specimens were ground with silicon carbide abrasive papers (grit 50–2000) and polished using 1 μm and 0.5 μm diamond pastes. Carbides were revealed using a 10 % ammonium persulfate solution heated to 70 °C, while pearlite and ferrite were etched with 4 % nital. Graphite nodules were examined on polished surfaces. Microstructures were characterized using a Nikon optical microscope and a Jeol-IT700HR scanning electron microscope, and phase quantification was performed by image analysis.

Pearlite interlamellar spacing was measured following the method of Voort et al. [14], in which a circle is placed on a high-magnification micrograph and the number of intersections with cementite lamellae is counted. The spacing was then calculated using Eq. (1), where S is the average pearlite interlamellar spacing, D the circle diameter, n the number of intersections, and M the magnification.

$$S = \frac{\pi D}{nM} \tag{1}$$

Nodule morphology and distribution were analyzed using several parameters. The interparticle distance, which represents the carbon diffusion distance, was calculated using Eq. (2) [15].

$$\lambda_G = (55.4)\left(\frac{Ns_{avg}}{Perimeter^2}\right)^{1/3} \tag{2}$$

Nodule size was determined using Eq. (3) [16], considering only particles with diameters greater than 10 μm.

$$NS_{avg} = (2)\left(\sqrt{A\pi^{-1}}\right) \tag{3}$$

Nodularity was defined as the percentage of spheroidal graphite relative to the total graphite and was calculated using Equations (4) and (5) [15]. Equation (4) provides the sphericity index, where only particles with values greater than 0.65 were considered spheroidal; these particles were then used in Equation (5) to obtain the nodularity.

$$\%SSF = \frac{4 \cdot \pi \cdot Area}{Perimeter^2} \tag{4}$$

$$\%Nod = \left(\frac{Area\ \ of\ \ acceptable\ \ particles}{Area\ \ of\ \ acceptable + unacceptable\ \ particles}\right) \cdot 100 \tag{5}$$

Mechanical properties evaluated included hardness, impact toughness, wear resistance, elongation, UTS and YS. Hardness was measured on the Rockwell C scale using a 150 kgf load and a diamond indenter. Ten measurements were taken per alloy from specimens 1 in. thick with parallel polished surfaces. Impact toughness was assessed by Charpy testing according to ASTM E23 [17], using three specimens per alloy. Wear resistance was evaluated following ASTM G77-05 using a TE 53 Slim multi-purpose friction and wear tester under

https://doi.org/10.64486/m.65.3.1

a 50 N load, 300 rpm speed and 400 revolutions in dry sliding. Wear scar dimensions were measured, and volume loss was calculated using Eq. (6) [18].

$$lost\ \ volume = \frac{D^2 t}{8}\left[2sen^{-1}\frac{b}{D} - sen\ \ \left(2sen^{-1}\frac{b}{D}\right)\right] \quad (6)$$

Tensile testing was carried out using an Instron Series 3400 universal testing machine according to ASTM E8/E8M [19]. Elongation, UTS and YS values correspond to the average of three tests per alloy.

3. Results and discussion

3.1. Ductile iron composition

The chemical compositions of the four alloys are listed in Table 1. The carbon equivalent (CE) was calculated using Eq. (7) [20], incorporating the carbon, silicon and phosphorus contents. All four alloys lie within the hypereutectic composition range. Maintaining a CE below 4.65 % is known to enhance the distribution and morphology of graphite nodules, which contributes to improved consistency in mechanical performance [21]. Sulfur and phosphorus contents remained below 0.011 % and 0.009 %, respectively. The low sulfur concentration enabled the formation of stable graphite nodules uniformly distributed within the metallic matrix. This promoted higher nodularity, which in turn enhanced ductility and impact toughness [22]. Conversely, maintaining phosphorus levels below critical thresholds prevented grain boundary segregation and the formation of phosphide eutectic (steadite), a brittle phase commonly associated with reduced toughness. These compositional conditions contributed to a more favorable microstructural morphology, directly influencing the mechanical performance of the alloys [23].

$$CE = \%C + \frac{1}{3}(\%Si + \%P) \quad (7)$$

Table 1. Chemical composition of the four ductile iron alloys

Element % wt.	Alloy 1	Alloy 2	Alloy 3	Alloy 4
C	3.76	3.62	3.71	3.67
Si	2.54	2.64	2.51	2.61
Mn	0.38	0.32	0.37	0.32
S	0.011	0.01	0.008	0.009
P	0.009	0.007	0.006	0.009
Nb	0	0.11	0.23	0.32
CE	4.60	4.50	4.55	4.54

3.2. Metallographic analysis

Figure 1 shows the microstructural phases of the alloys. In the upper images, ferrite and pearlite are observed: bright regions correspond to ferrite, which provides higher toughness and elongation, while dark regions correspond to pearlite, which offers greater hardness and wear resistance. The central images, obtained by scanning electron microscopy, reveal the pearlite lamellae, where cementite appears as white lamellae and ferrite as dark lamellae. Previous studies have shown that small niobium additions refine pearlite by decreasing the interlamellar spacing. This effect is mainly attributed to two factors: (I) delayed eutectoid transformation and Nb segregation in austenite, which promote pearlite nucleation and limit carbon diffusion; and (II) NbC precipitation, which provides nucleation sites and restricts lamellar growth.

In the lower part of Figure 1, NbC carbides are observed, primarily along austenite grain boundaries, where they form interconnected networks. These carbides increase hardness and tensile strength but reduce toughness and elongation by interrupting the continuity of the metallic matrix.

https://doi.org/10.64486/m.65.3.1

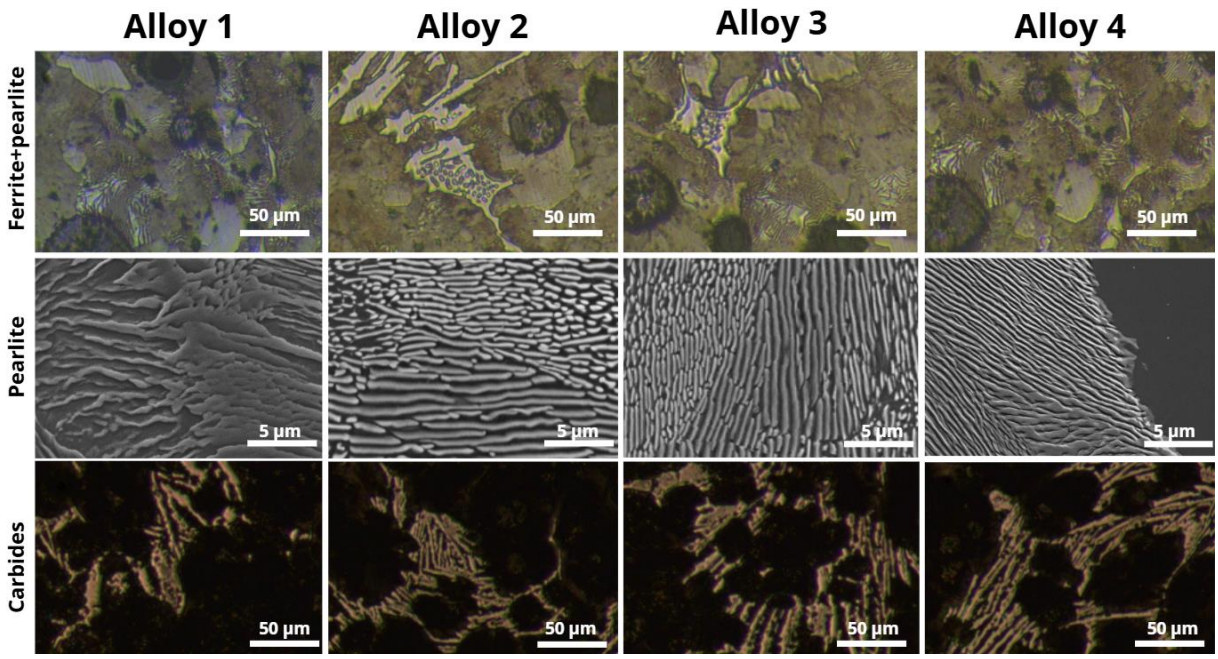

Figure 1. Micrographs of the four alloys showing the different microstructures

Table 2 summarizes the quantitative analysis of phases and nodule features. Niobium increased the pearlite fraction from 25.44 % in the niobium-free alloy to 73.31 % in Alloy 4. This behavior is related to the reduced carbon diffusion caused by Nb, which delays ferrite formation and promotes pearlite. The NbC content also rose from 0.53 % in Alloy 1 to 2.48 % in Alloy 4. NbC particles act as barriers to carbon diffusion and limit the growth of pearlite colonies. Similarly, the presence of Nb in solid solution within austenite exerts a solute-drag effect that reduces the mobility of carbon atoms, thereby delaying the austenite-to-pearlite transformation and promoting the nucleation of a finer microstructure [24].

Table 2. Graphite morphology and phase distribution average in alloys with varying niobium content

Characteristics	Alloy 1	Alloy 2	Alloy 3	Alloy 4
Nodule size/µm	21.72	29.96	26.56	23.23
Nodularity/%	87.23	81.5	81.65	81.9
Nodule count nod/mm^2	256.1	113.7	120.4	156.4
Interparticle distance µm	23.92	35.51	33.51	29.33
Graphite/%	8.00	6.95	6.11	6.665
Carbides/%	0.53	0.95	1.51	2.48
Pearlite/%	25.44	63.17	75	73.31
Ferrite/%	66.03	23.42	17.38	17.54
Pearlite lamellar Spacing/µm	1.21	0.82	0.76	0.73

Consequently, ferrite and cementite lamellae exhibited a reduced interlamellar spacing, decreasing from 1.21 µm in Alloy 1 to 0.73 µm in Alloy 4, which increased the density of interfaces and resulted in a refined microstructure. Regarding graphite nodules, niobium reduced carbon availability due to carbide formation, limiting new nodule nucleation. As a result, the nodule count and nodularity decreased from 256.1 nod/mm^2 and 87.23 % in Alloy 1 to 156.4 nod/mm^2 and 81.9 in Alloy 4. At the same time, lower nodule density promoted the growth of existing nodules, increasing their size from 21.72 µm to 23.23 µm.

https://doi.org/10.64486/m.65.3.1

The reduced nucleation sites also produced a wider nodule distribution, increasing interparticle distance from 23.92 μm in Alloy 1 to 35.51 μm in Alloy 2.

3.3. Mechanical tests

Figure 2 presents the mechanical test results. Hardness increased from 13.72 HRC in Alloy 1 to 26.6 HRC in Alloy 4. This improvement is attributed to (I) the larger pearlite fraction, which is harder than ferrite, and (II) the formation of NbC carbides, which are significantly harder than the metallic matrix. NbC also contributed to pearlite refinement, strengthening the matrix through the Hall–Petch mechanism [25].

Impact toughness decreased with increasing niobium, from 10.45 J in Alloy 1 to 5 J in Alloy 4. This reduction is associated with the higher fractions of hard and brittle phases, such as pearlite and NbC, which act as crack-initiation sites. In addition, the lower nodule density and higher interparticle distance reduced the ability of graphite nodules to deflect cracks, facilitating faster propagation.

UTS and YS increased, reaching 746 MPa and 449 MPa, respectively, in Alloy 4. This strengthening is due to the combined effects of a higher pearlite fraction and the dispersion of NbC, which hinders dislocation motion and provides dispersion strengthening. In contrast, elongation decreased from 8.92 % in Alloy 1 to 4.02 % in Alloy 4. The reduction is attributed to the prevalence of hard, less ductile phases (pearlite and NbC), along with lower nodule counts and larger interparticle distances, which promote stress concentration and early fracture. Wear resistance improved with increasing niobium. Volume loss decreased due to the higher pearlite fraction, which increased matrix hardness, and the presence of NbC carbides, which acted as local reinforcements against abrasion. Additionally, although nodule density decreased, the larger and more widely spaced nodules helped limit microcrack propagation around their boundaries, delaying severe wear.

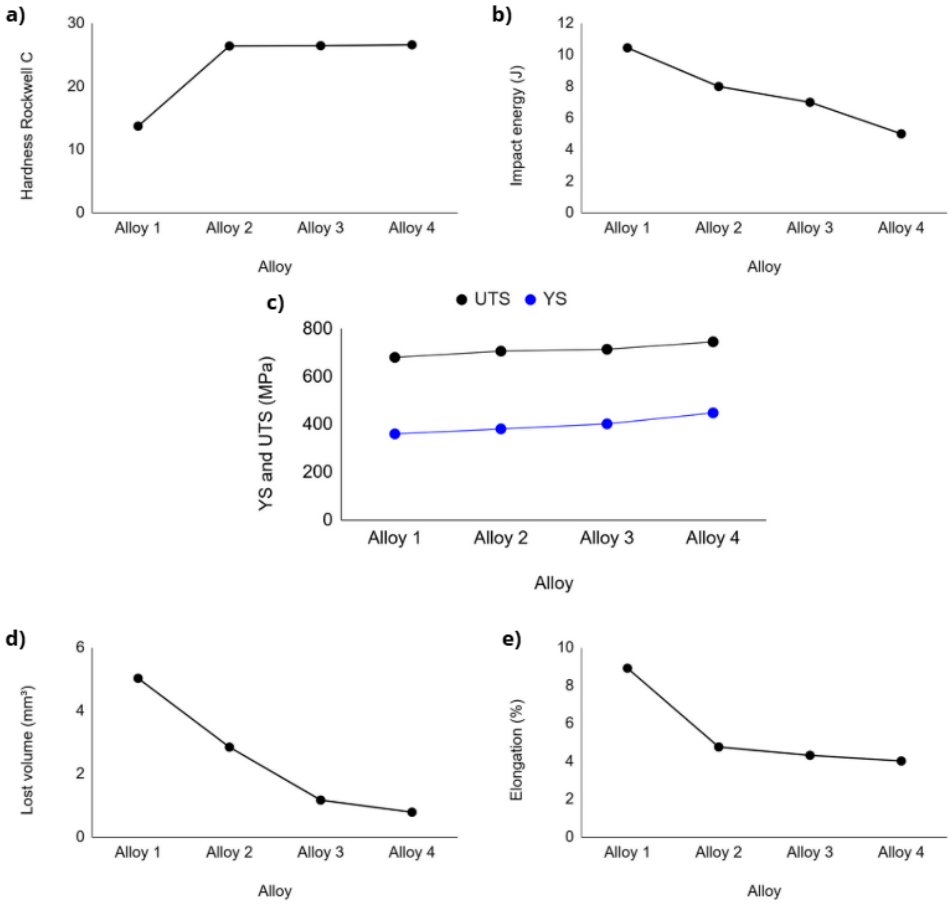

Figure 2. Results of the mechanical tests applied to the alloys: a) Hardness test, b) Charpy impact test, c) UTS and YS, d) Volume loss during the wear test, and e) Percentage of elongation..

https://doi.org/10.64486/m.65.3.1

4. Conclusions

This study evaluated the role of niobium as an alloying element in ductile iron, with emphasis on microstructural evolution and mechanical behavior. Niobium additions promoted the formation of pearlite and NbC carbides, leading to higher hardness, tensile strength and wear resistance. The best combination of hardness and wear resistance was achieved in the alloy containing 0.32 wt.% Nb, while the highest impact energy was observed in the niobium-free alloy due to its higher ferrite fraction and larger nodule count. Overall, niobium enhances strength and wear resistance, but at the expense of toughness.

Acknowledgments: The authors would like to express their sincere gratitude to the Secretaría de Ciencia, Humanidades, Tecnología e Innovación (SECIHTI) and the Universidad Autónoma del Estado de Hidalgo (UAEH) for their generous support, which was essential to the successful development of this research work.

References

[1] W. Sckudlarek, M. N. Krmasha, K.S. Al-Rubaie et al., "Effect of austempering temperature on microstructure and mechanical properties of ductile cast iron modified by niobium," *Journal of Materials Research and Technology*, vol 12, pp. 2414-2425, May. 2021, https://doi.org/10.1016/j.jmrt.2021.04.041.

[2] O.J. Akinribide, S.O.O. Olunsunle, S.O. Akinwamide et al., "Impact of heat treatment on mechanical and tribological behavior of unalloyed and alloyed ductile iron," *Journal of Materials Research and Technology*, vol. 14, pp. 1809-1819, Sep. 2021, https://doi.org/10.1016/j.jmrt.2021.07.077.

[3] B. Wang, L. Zhao, Y. Chen et al., "Intelligent corrosion analysis and life prediction of ductile iron pipe systems using machine learning and electrochemical sensors," *Journal of Materials Research and Technology*, vol. 33, pp. 725-741, Nov. 2024, https://doi.org/10.1016/j.jmrt.2024.09.076.

[4] M. Medeiros, G. Vieira, A. Froehlich et al., "Microstructure and mechanical properties of SiMo ductile cast irons alloys with varied Mo and Nb contents," *Journal of Materials Research and Technology*, vol 30, pp. 6301-6308, May. 2024, https://doi.org/10.1016/j.jmrt.2024.05.029.

[5] S.K. Alias, B. Abdullah, A. Jaffar et al., "Development of High Strength Ductile Iron with Niobium Addition," *Advanced Materials Research*, vol 576, pp. 366-369, Oct. 2012, https://doi.org/10.4028/www.scientific.net/AMR.576.366.

[6] S. Pan, F. Zeng, N. Su et al., "The effect of niobium addition on the microstructure and properties of cast iron used in cylinder head," *Journal of Materials Research and Technology*, vol. 9, no. 2, pp. 1509-1518, Mar. 2020, https://doi.org/10.1016/j.jmrt.2019.11.076.

[7] A. Bedolla, E. Solis and B. Hernandez, "Effect of niobium in medium alloyed ductile cast irons," *International Journal of Cast Metals Research*, vol. 16, no. 5, pp. 481-486, 2003, https://doi.org/10.1080/13640461.2003.11819625.

[8] Z. Wenbin, Z. Hongbo, Z. Dengke et al., "Nb alloying effect in high carbon equivalent grey cast iron," *China Foundry*, vol. 1, no. 8, pp. 36-40, 2011. https://www.researchgate.net/publication/286666747_Niobium_alloying_effect_in_high_carbon_equivalent_grey_cast_iron

[9] D.H. Munhoz and O. Petri, "Niobium effects on properties of austempered ductile iron- ADI," *American Journal of Engineering Research (AJER)*, vol. 7, no.7, pp. 181-193, Jul. 2018. https://www.researchgate.net/publication/326424102_Niobium_Effects_On_Properties_Of_Austempered_Ductile_Iron-ADI

[10] E.M. Fras, M. Gorny and M. Kawalec, "Effect of small additions of vanadion and niobium on structure and mechanical properties of ductile iron," *Archives of Foundry Engineering*, vol. 7, no. 1, pp. 89-92, 2007. https://www.researchgate.net/publication/313139113_

[11] Effect_of_small_additions_of_vanadion_and_niobium_on_structure_and_mechanical_properties_of_ductile_iron
T. Souza and R. Nogueira, ""Mechanical and microstructural characterization of nodular cast iron (NCI) with niobium additions," *Materials Research*, vol. 17, no. 5, pp. 1167-1172, Oct. 2014. https://doi.org/10.1590/1516-1439.249413.

[12] X. Chen, J. Xu, H. Hu et al., "Effects of niobium addition on microstructure and tensile behavior of as-cast ductile iron," *Materials Science and Engineering: A*, vol. 688, pp. 416-428, Mar. 2017, https://doi.org/10.1016/j.msea.2017.01.032.

[13] A.S. Pimentel, W.L. Guesser, W.J. da Silva et al., "Abrasive wear behavior of austempered ductile iron with niobium additions," *Wear*, vol. 440-441, art no. 203065, Dec. 2019, https://doi.org/10.1016/j.wear.2019.203065.

[14] G.F. Voort and A. Roosz, "Measurement of the interlamellar spacing of pearlite," *Metallography*, vol. 17, no. 1, pp. 1-17, Feb. 1984, https://doi.org/10.1016/0026-0800(84)90002-8.

[15] R.E. Ruxanda, D.M. Stefanescu and T.S. Piwonka, "Microstructure Characterization of Ductile Thin-Wall Iron Castings," *AFS Transaction*, vol. 110, pp. 1-17, Apr. 2002. https://www.researchgate.net/publication/260713346_Microstructure_Characterization_of_Ductile_Thin_Wall_Iron_Castings

[16] K.M. Pedersen and N. Tiedje, "Solidification of Hypereutectic Thin Wall Ductile Cast Iron," *Materials Science Forum*, vol. 508, pp. 63-68, Mar. 2006, https://doi.org/10.4028/www.scientific.net/MSF.508.63.

[17] ASTM International, "ASTM E23-24: Métodos de prueba estándar para pruebas de impacto de barras con entalla de materiales metálicos," ASTM International, 2024. [Online]. Available: https://doi.org/10.1520/E0023-24 [Accessed: Aug. 5, 2025].

[18] ASTM International, "ASTM G77-05: Standard Test Method for Ranking Resistance of Materials to Sliding Wear Using Block-on-Ring Wear Test," ASTM International, 2005. [Online]. Available: https://doi.org/10.1520/G0077-05 [Accessed: Aug. 8, 2025].

[19] ASTM International, "ASTM E8/E8M-21: Standard Test Methods for Tension Testing of Metallic Materials," ASTM International, 2021. [Online]. Available: https://doi.org/10.1520/E0008_E0008M-21 [Accessed: Aug. 11, 2025].

[20] A. Cruz, E. Colín, J. Chávez et al., "Evaluation of CADI Low Alloyed with Chromium for Camshafts Application," *Metals*, vol. 12, no. 2, pp. 249, 2022, https://doi.org/10.3390/met12020249.

[21] C.I. García, K. Cho, K. Redkin et al., "Influence of critical carbide dissolution temperature during intercritical annealing on hardenability of austenite and mechanical properties of DP-980 steels," *ISIJ International*, vol. 51, no. 6, pp. 969-974, 2011, http://dx.doi.org/10.2355/isijinternational.51.969.

[22] S. Boonmee and N. Mai, "Effect of Sulfur on the Formation of the Graphite Degradation in Ductile Iron," *Materials Science Forum*, vol.895, pp. 89-93, Mar. 2017, https://doi.org/10.4028/www.scientific.net/MSF.895.89.

[23] A. Sambas, G. Ananto and S. Gunara, " Analyze the effect of phosphorus on the mechanical properties and microstructure on cast iron," *MATEC*, vol. 204, 2018, http://dx.doi.org/10.1051/matecconf/201820405008.

[24] H. Wang, Y. Feng, W. Jiang et al., "Effect of Niobium on Microstructure and Mechanical Properties of Ductile Iron with High Strength and Ductility," *Journal of Materials Engineering and Performance*, vol. 33, pp. 896-905, 2024, https://doi.org/10.1007/s11665-023-08019-9.

[25] S.N. Naik and S.M. Walley, "The Hall–Petch and inverse Hall–Petch relations and the hardness of nanocrystalline metals," *Journal of Materials Science*, vol 55, pp. 2661-2681, 2020, https://doi.org/10.1007/s10853-019-04160-w.

https://doi.org/10.64486/m.65.3.1